

Using Biofunctionalized Nanoparticles To Probe Pathogenic Bacteria

Kun-Chan Ho,[†] Pei-Jane Tsai,[‡] Ya-Shiuan Lin,[†] and Yu-Chie Chen^{*†}

Department of Applied Chemistry, National Chiao Tung University, Hsinchu 300, Taiwan, and
Department of Laboratory Medicine and Biotechnology, Tzu-Chi University, Hualien 970, Taiwan

In this paper, we report a method for fabricating biofunctionalized nanoparticles by attaching human immunoglobulin (IgG) onto their surfaces through either electrostatic interactions or covalent binding. We found that these IgG-presenting nanoparticles can bind selectively to the cell walls of pathogens that contain IgG-binding sites based on the investigation of transmission electron microscopy images. Our results demonstrate that such Au–IgG nanoparticles may serve as useful nanoscale probes for exploring the interactions between IgG and pathogens. Furthermore, the IgG-presenting magnetic nanoparticles have been employed as effective affinity probes for selectively concentrating traces of target bacteria from sample solutions. The trapped bacteria were then characterized by using matrix-assisted laser desorption/ionization mass spectrometry. The lowest cell concentration we detected for both *Staphylococcus saprophyticus* and *Staphylococcus aureus* in aqueous sample solutions (0.5 mL) was $\sim 3 \times 10^5$ cfu/mL, while the detectable cell concentration for *S. saprophyticus* in a urine sample was $\sim 3 \times 10^7$ cfu/mL.

Biomolecule-functionalized nanoparticles have been demonstrated previously as suitable probes for investigating specific recognition processes between microorganisms and biomolecules.¹² Thiol–metal interactions and amide bond formation are frequently used to bind biomolecules covalently onto the surfaces of nanoparticles; for instance, Lin et al.¹ employed mannose-functionalized gold nanoparticles as nanoscale probes that recognize the pili in *Escherichia coli*, and Gu et al.² bound vancomycin covalently to the surfaces of magnetic nanoparticles, which they employed for the capture of pathogens, through S–Pt bonding. In this paper, we propose an alternative, simple method for nanofabricating protein-functionalized gold nanoparticles by taking advantage of the electrostatic interactions between these charged species. Because amphiprotic species, such as peptides and proteins, have unique isoelectric points (pI), when the pH of a

protein sample solution is lower than the value of the pI of the protein, the protein molecules have net positive charges. Citrate-functionalized, anionically charged gold nanoparticles tend to attract positively charged protein molecules onto their surfaces through electrostatic interactions.³ Varying the pH of the solution provides a simple method for controlling the presentation of positively charged proteins onto the negatively charged surfaces of gold nanoparticles.

Human immunoglobulin G (IgG) is a well-known target protein for several pathogenic bacteria.⁴ For instance, it can be used to study the interactions between IgG and protein A on the cell walls of *Staphylococcus aureus*; this specific binding affinity was discovered almost 40 years ago.⁴ Protein A binds selectively to the Fc region of IgG in a process that is usually called a pseudoimmune reaction, as opposed to the specific binding of an antigen at antibody Fab sites.⁵ Based on this unique example of biomolecular recognition, protein A affinity sorbents have been employed extensively for the purification of IgG from human serum.^{6–8} The ability of IgG to recognize protein A motivated us to develop IgG-presenting nanoparticles as recognition probes for pathogens whose cell walls display IgG binding sites; by developing such a system we would be able to explore the interactions between IgG and the cell walls of bacteria. Typically, the isoelectric point of IgG is close to 7,⁹ which means that IgG molecules bear a net positive charge in solution at pH 6. Gold nanoparticles that have negatively charged surfaces at pH 6 can be generated from the reduction of tetrachloroaurate (0.1 mg/mL, 50 mL) using trisodium citrate (1%, 1 mL) while stirring vigorously at 100 °C.¹⁰

Additionally, we have also functionalized magnetic nanoparticles through covalently bonding immobilizing IgG onto the surfaces of the nanoparticles to generate affinity probes that concentrate traces of target bacteria from sample solutions. The magnetic particles that conjugate with the target bacteria are then very readily isolated from the solution by applying an external magnet. We characterized the trapped bacteria by using matrix-

* Corresponding author. E-mail: yuchie@mail.nctu.edu.tw. Phone: 886-3-5131527. Fax: 886-3-5744689.

[†] National Chiao Tung University.

[‡] Tzu-Chi University.

- (1) Lin, C.-C.; Yeh, Y.-C.; Yang, C.-Yi.; Chen, C.-L.; Chen, G.-F.; Chen, C.-C.; Wu, Y.-C. *J. Am. Chem. Soc.* **2002**, *124*, 3508–3509.
- (2) Gu, H.; Ho, P.-L.; Tsang, K. W. T.; Wang, L.; Xu, B. *J. Am. Chem. Soc.* **2003**, *125*, 15702–15703.

(3) Teng, C.-H.; Ho, K.-C.; Lin, Y.-S.; Chen, Y.-C. *Anal. Chem.* **2004**, *76*, 4337–4342.

(4) Forsgren, A.; Sjöquist, J. *J. Immunol.* **1966**, *97*, 822–827.

(5) Langone, J. L. *Adv. Immunol.* **1982**, *32*, 157–252.

(6) Ankerst, J.; Christensen, P.; Kjellén, L.; Kronvall, G. *J. Infect. Dis.* **1974**, *130*, 268–273.

(7) Chantler, S.; Devries, E.; Allen, P. R.; Huen, A. L. *J. Immunol. Methods* **1976**, *13*, 367–380.

(8) Hahn, R.; Schlegel, R.; Jungbauer, A. *J. Chromatogr., B* **2003**, *790*, 35–51.

(9) Ai, H.; Fang, M.; Jones, S. A.; Lvov, Y. M. *Biomacromolecules* **2002**, *3*, 560–564.

(10) Frens, G. *Nat. Phys. Sci.* **1973**, *241*, 20–22.

assisted laser desorption/ionization mass spectrometry (MALDI-MS). MALDI-MS is a useful tool for the characterization of microorganisms.^{14–28} Combining Fe–IgG nanoscale probes with MALDI-MS can allow the rapid identification of microorganism species.

EXPERIMENTAL SECTION

Reagents. Iron(III) chloride hexahydrate and trisodium citrate were purchased from Riedel-de Haën (Seelze, Germany), and iron(II) chloride tetrahydrate was obtained from Aldrich (Milwaukee, WI). Ammonium hydroxide was obtained from J. T. Baker (Phillipsburg, NJ). Gold(III) chloride hydrate was obtained from Showa (Tokyo, Japan). Sodium phosphate monobasic was obtained from Mallinckrodt. Sodium phosphate dibasic heptahydrate, IgG from human serum, protein G, bovine serum albumin (BSA), *N*-(3-dimethylaminopropyl)-*N'*-ethylcarbodiimide hydrochloride, and 3,5-dimethoxy-4-hydroxycinnamic acid (sinapinic acid) were obtained from Sigma (St. Louis, MO). Protein A was purchased from Fluka (Steinheim, Germany). Hydrochloric acid, sodium hydroxide, and trifluoroacetic acid were obtained from Merck (Darmstadt, Germany). Luria Bertani (LB) broth was obtained from Athena Enzyme System. Potato Dextrose Agar was purchased from Difco.

Preparation of Bacterial Samples. *S. aureus* and *Staphylococcus saprophyticus* were collected from patients at the General Tzu-Chi Hospital, Hualien, Taiwan. *Streptococcus pyogenes* JRS 75 and JRS 4 were kind gifts from Dr. J. R. Scott. *S. pyogenes* JRS 75 was obtained by mutating M protein from the strain of *S. pyogenes* JRS 4.²⁹ *S. saprophyticus*, *S. pyogenes*, and *S. aureus* were cultured

in 15 mL of LB broth (25 g/L). After incubation overnight at 37 °C, the bacterial cells were centrifuged at 6000 rpm for 10 min. The bacteria were washed with sterilized water (2 × 10 mL). The bacteria were then heat-killed in a water bath (100 °C) for 30 min. The desired bacterial concentration was adjusted by measuring the optical density at 600 nm, and it was checked by plating serial dilutions of the samples on potato dextrose agar and counting the colony forming unit (cfu) after incubation overnight at 37 °C. In the experiment using live bacteria, the bacterial cells were used directly as the sample without heat treatment. Similarly, the desired bacterial concentration was prepared based on the measurement of the optical density at 600 nm.

Preparation of IgG–Au Nanoparticles. An aqueous tetrachloroaurate solution (0.1 mg/mL, 50 mL) was heated to its boiling point, and then trisodium citrate (1%, 1 mL) was added to the solution while stirring. The color change of the solution from blue to brilliant red indicated the formation of monodispersed spherical particles (~16 nm). The surfaces of gold nanoparticles presented citrate anions, which bound strongly through ionic interactions. The value of *pI* of IgG is close to 7.0, and therefore, in a solution at pH 6.0, IgG should bear a net positive charge. Thus, when the IgG (pH 6.0) solution was mixed with the gold nanoparticle solution, IgG should become attached onto the surfaces of gold nanoparticles through ionic interactions. The mixture of IgG (25 µg/mL, 0.5 mL) and gold nanoparticles (0.5 mL) was incubated at room temperature for 30 min to generate the Au–IgG nanoparticles. We used UV–visible absorption spectroscopy to examine whether the IgG units had become attached to the gold nanoparticle surfaces. Because the absorption capacity of IgG at a concentration of 25 µg/mL in the UV–visible region was too low, the amounts of IgG and gold nanoparticles we used in the UV–visible absorption experiment were 10 times higher than those used in the actual experiments to fabricate the Au–IgG nanoparticles. The concentrated gold nanoparticle solution was prepared by centrifuging 5 mL of the gold nanoparticle solution (prepared as described above) at 13 000 rpm for 30 min and then removing the supernatant (4.5 mL). The gold nanoparticles were then resuspended into the remaining solution (0.5 mL) under gentle vortex mixing. For the UV–visible measurements, we mixed 0.5 mL of 250 µg/mL IgG with 0.5 mL of the concentrated gold nanoparticle solution. After incubation for 20 min, the supernatant obtained after centrifugation of the Au–IgG incubation solution was examined using UV–visible absorption spectroscopy; Figure 1 presents the results. The solid line represents the absorption of the supernatant solution obtained after centrifugation of the IgG–Au incubation solution. The dotted line represents the UV absorption of the IgG solution (250 µg/mL). The intensity of the absorption of the IgG obtained from the supernatant after centrifugation of the IgG–Au mixture is obviously lower than that of the initial IgG solution. These results indicate that the IgG molecules had attached to the surfaces of the gold nanoparticles.

Preparation of Au–BSA Nanoparticles. The value of *pI* of BSA is 5.8, and therefore, in a phosphate buffer solution at pH 5.5, BSA should bear a net positive charge. A mixture of the BSA solution (25 µg/mL, pH 5.5, 0.5 mL) and the gold nanoparticles solution (0.5 mL), obtained as described above, was incubated

- Brandt, E. R.; Hayman, W. A.; Currie, B.; Carapetis, J.; Wood, Y.; Jackson, D. C.; Cooper, J.; Melrose, W. D.; Saul, A. J.; Good, M. F. *Immunology* **1996**, *89*, 33–337.
- Koneracká, M.; Kopčanský, P.; Antalík, M.; Timko, M.; Ramchand, C. N.; Lobo, D.; Mehta, R. V.; Upadhyay, R. V. *J. Magn. Magn. Mater.* **1999**, *201*, 427–430.
- Claydon, M. A.; Davey, S. N.; Edwards-Jones, V.; Gordon, D. B. *Nat. Biotechnol.* **1996**, *14*, 1584–1586.
- Holland, R. D.; Wilkes, J. G.; Rafii, F.; Sutherland, J. B.; Persons, C. C.; Voorhees, K. J.; Lay, J. O., Jr. *Rapid Commun. Mass Spectrom.* **1996**, *10*, 1227–1232.
- Liang, X.; Zheng, K.; Qian, M. G.; Lubman, D. M. *Rapid Commun. Mass Spectrom.* **1996**, *10*, 1219–1226.
- Krishnamurthy, T.; Ross, P. L. *Rapid Commun. Mass Spectrom.* **1996**, *10*, 1992–1996.
- Welham, K. J.; Domin, M. A.; Scannell, D. E.; Cohen, E.; Ashton, D. S. *Rapid Commun. Mass Spectrom.* **1998**, *12*, 176–180.
- Wang, Z.; Russon, L.; Li, L.; Roser, D. C.; Long, S. R. *Rapid Commun. Mass Spectrom.* **1998**, *12*, 456–464.
- Easterling, M. L.; Colangelo, C. M.; Scott, R. A.; Amster, I. J. *Anal. Chem.* **1998**, *70*, 2704–2709.
- Arnold, R. J.; Reilly, J. P. *Rapid Commun. Mass Spectrom.* **1998**, *12*, 630–636.
- Lynn, E. C.; Chung, M.-C.; Tsai, W.-C.; Han, C.-C. *Rapid Commun. Mass Spectrom.* **1999**, *13*, 2022–2027.
- Nilsson, C. L. *Rapid Commun. Mass Spectrom.* **1999**, *13*, 1067–1071.
- Dai, Y.; Li, L.; Roser, D. C.; Long, S. R. *Rapid Commun. Mass Spectrom.* **1999**, *13*, 73–78.
- Winkler, M. A.; Uher, J.; Cepa, S. *Anal. Chem.* **1999**, *71*, 3416–3419.
- Demirev, P. A.; Ho, Y.-P.; Ryzhov, V.; Fenselau, C. *Anal. Chem.* **1999**, *71*, 2732–2738.
- Li, T.-Y.; Liu, B.-H.; Chen, Y.-C. *Rapid Commun. Mass Spectrom.* **2000**, *14*, 2393–2400.
- Fenselau, C.; Demirev, P. A. *Mass Spectrom. Rev.* **2001**, *20*, 157–171.
- Lazar, L. M.; Ramsey, R. S.; Ramsey, J. M. *Anal. Chem.* **2001**, *73*, 1733–1739.
- Norgren, M.; Caparon, M. G.; Scott, J. R. *Infect. Immun.* **1989**, *57*, 3846–3850.

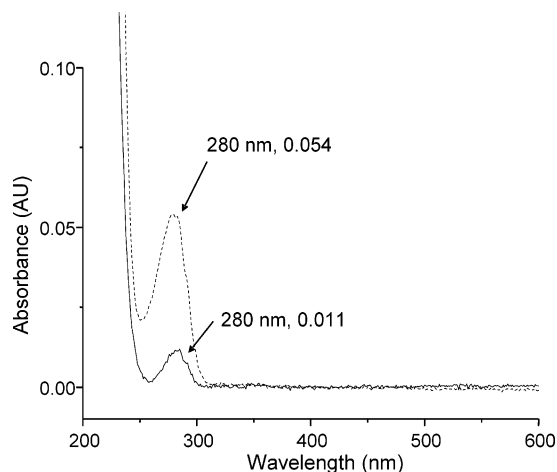


Figure 1. UV-visible absorption spectra of IgG (250 $\mu\text{g/mL}$, dotted line) and the supernatant of the incubated Au-IgG solution (solid line) after centrifugation.

for 30 min at room temperature to generate Au-BSA nanoparticles.

Using Nanoparticles To Probe Target Bacteria. An Au-IgG solution (1 mL), prepared as described above, was added to 0.5 mL of an aqueous bacteria solution ($\sim 10^7$ cells/mL). The mixture was incubated at $-20\text{ }^\circ\text{C}$ for 15 min and then at room temperature for another 30 min. Control experiments were performed by using Au-BSA and unmodified gold nanoparticles as the probes. Similarly, Au-BAS (or Au) nanoparticles (1 mL) were added into 0.5 mL of an aqueous bacteria solution ($\sim 10^7$ cells/mL), and the mixture was incubated at $-20\text{ }^\circ\text{C}$ for 15 min and then at room temperature for another 30 min.

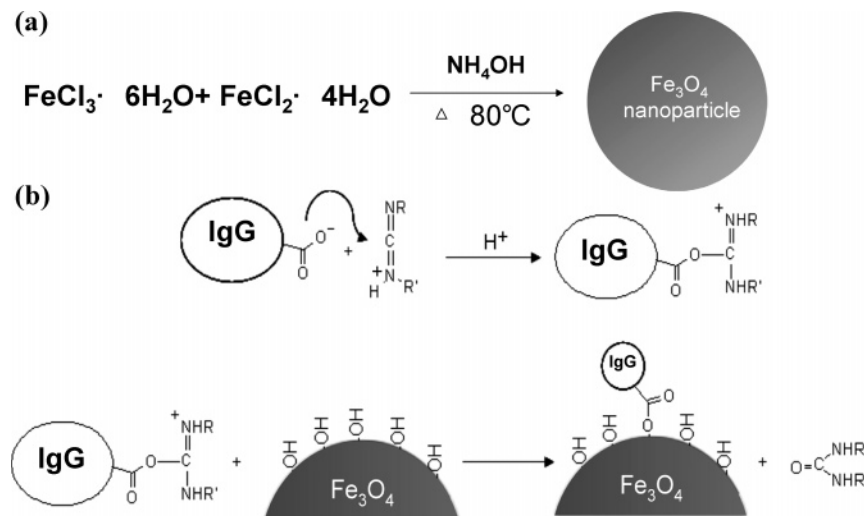
Preparation of Transmission Electron Microscopy (TEM) Samples. The sample solutions obtained above were centrifuged at 2100 rpm. Most of the bacterial cells settled at the bottom of the sample vial, but the nanoparticles remained suspended in the solution under these centrifugation conditions unless they were bound to the cell walls of the bacterial cells or became large particles as a result of aggregation. The supernatant was then discarded after centrifugation. The remaining bacterial cells conjugated with nanoparticles were washed twice with deionized

water (0.5 mL) under gentle vortex mixing for 10 min. The supernatant was then discarded after centrifugation (2100 rpm). The remaining bacterial cells that might be conjugated with the nanoparticles were then resuspended in deionized water (0.5 mL). After gentle vortex mixing for another 10 min, 2 μL of this suspension solution was deposited on the copper holder of a TEM. After drying, the sample was ready for TEM analysis.

Preparation of Magnetic Nanoparticles. Magnetic Fe_3O_4 nanoparticles were prepared by stirring $\text{FeCl}_3 \cdot 6\text{H}_2\text{O}$ (5.4 g), $\text{FeCl}_2 \cdot 4\text{H}_2\text{O}$ (1.98 g), and deionized water (20 mL) in a water bath maintained at $80\text{ }^\circ\text{C}$, and then aqueous NH_4OH solution (8 M, 15 mL) was added into the $\text{FeCl}_3/\text{FeCl}_2$ mixture until a black precipitate appeared.¹² The mixture was stirred continuously for 30 min in the water bath maintained at $80\text{ }^\circ\text{C}$. When the reaction was complete, the magnetic particles in the sample solution were aggregated onto the wall of the sample vial by positioning a magnet (magnetic field, $\sim 5000\text{ G}$) at the edge of the vial. The remaining solution was then removed by pipet. The isolated magnetic nanoparticles were washed repeatedly with hot water to remove any unreacted impurities. The magnetic particles were dried in an oven at $120\text{ }^\circ\text{C}$ for 30 min.

Preparation of IgG-Immobilized Magnetic Nanoparticles. Scheme 1 presents the synthetic route we followed to immobilize IgG onto the surfaces of Fe_3O_4 magnetic nanoparticles. IgG (1 mg) was dissolved in a phosphate-buffered saline solution (PBS, pH 6.3, 6 mL), which was prepared by dilution of Na_2HPO_4 (6.15 mL, 0.2 M) and NaH_2PO_4 (43.85 mL, 0.2 M) to 100 mL. Magnetic nanoparticle (3 mg) and *N*-(3-dimethylaminopropyl)-*N'*-ethylcarbodiimide hydrochloride (1 mg) were then added into the IgG solution. The mixture was vortexed for 24 h. After the reaction was complete, the product was aggregated onto the wall of the sample vial by applying a magnet externally to the vial. The remaining solution was discarded, and the magnetic particles were washed with phosphate buffer ($2 \times 6\text{ mL}$). The rinsed IgG-modified magnetic nanoparticles were resuspended in the PBS (6 mL). The number of IgG molecules bound to the surfaces of the magnetic nanoparticles was estimated using UV-visible absorption spectroscopy. Based on the relative absorption (at a wavelength of 280 nm) between a stock solution of IgG and the supernatant of the incubated Fe-IgG sample after centrifugation,

Scheme 1. Synthetic Route for Immobilizing IgG onto the Surfaces of Fe_3O_4 Magnetic Nanoparticles



we estimated that ~ 1.87 nmol of IgG was immobilized onto the surface of 1 mg of magnetic nanoparticles.

Preparation of Fe–Protein G–IgG Nanoparticles. To confirm that the target bacteria were bound to the Fc region of IgG, we prepared Fe–protein G–IgG nanoparticles. Similar to protein A, protein G is an IgG-binding protein that binds to the Fc sites of IgG molecules.⁵ Instead of using protein A, we used protein G to immobilize IgG onto the surface of the nanoparticles. Protein G (1 mg) was dissolved in PBS (pH 6.3, 5 mL) solution. Magnetic nanoparticles (3 mg) and *N*-(3-dimethylaminopropyl)-*N*'-ethylcarbodiimide hydrochloride (1.78 mg) were then added into the protein G solution. The mixture was vortexed for 24 h. After the reaction was complete, the product was aggregated onto the wall of the sample vial by applying a magnet externally to the vial. The remaining solution was discarded, and the magnetic particles were washed with phosphate buffer (2×5 mL). The rinsed protein G-modified magnetic nanoparticles were resuspended in PBS (5 mL). We used UV–visible absorption spectroscopy to estimate the number of protein G molecules bound to the surfaces of the magnetic nanoparticles. Based on the relative absorption (at a wavelength of 280 nm) between the stock solution of protein G and the supernatant of the incubated Fe–protein G sample after centrifugation, we estimate that ~ 2.26 nmol of protein G was immobilized onto the surface of 1 mg of the magnetic nanoparticles.

The Fe–protein G nanoparticles were added into an IgG solution (0.292 mg/mL, 5 mL) prepared in PBS (pH 6.3). The mixture was vortexed gently for 1 h. After vortexing, the magnetic particles were aggregated onto the bottom of the sample vial by applying a magnet externally at the bottom of the sample vial. The supernatant was separated from the magnetic particles by pipet, and the supernatant was centrifuged at 14 000 rpm for 20 min to eliminate any remaining solid particles. The absorption of the supernatant was measured by UV absorption spectroscopy. Based on the relative absorption intensity (at 280 nm) of the original IgG solution and the supernatant, we estimate that ~ 1.42 nmol of IgG molecules were immobilized onto the surfaces of the Fe–protein G nanoparticles (1 mg).

Using the Biofunctionalized Magnetic Nanoparticles To Probe Bacteria. A portion of the biofunctionalized magnetic nanoparticles (Fe–IgG or Fe–protein G–IgG, 60 μ L) was added into a bacterial solution (0.5 mL). After gentle vortex mixing for 1 h, the magnetic nanoparticles were separated from the solution by applying a magnet externally at bottom of the sample vial; this process caused the magnetic nanoparticles to aggregate at the bottom of the vial. The supernatant was removed by pipet. The isolated nanoparticles were then rinsed with deionized water to remove any unbound impurities. Subsequently, a MALDI matrix solution (2.0 μ L) was added to the remaining nanoparticles. After incubation for 15 min, a portion of this MALDI matrix solution (0.5 μ L) was applied onto a sample target. After the solvents were evaporated, the sample was placed into a MALDI mass spectrometer for analysis.

Instrumentation. All mass spectra were obtained using a Biflex III (Bruker) time-of-flight mass spectrometer equipped with a 337-nm nitrogen laser, a 1.25-m flight tube, and a sample target having the capacity to load 384 samples simultaneously. The accelerating voltage was set to 19 kV. TEM images were obtained

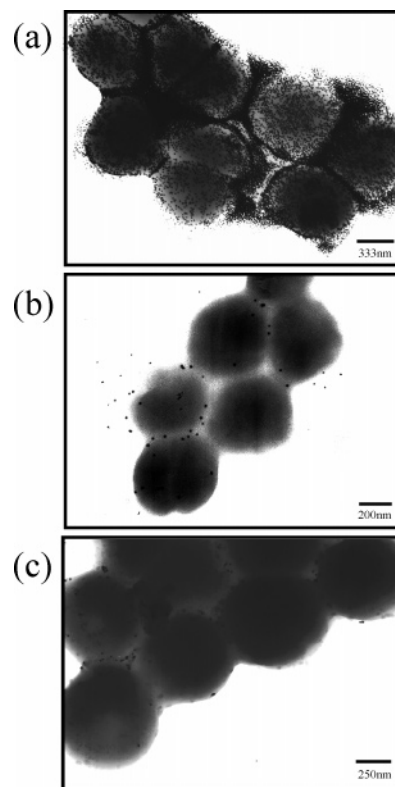


Figure 2. TEM images of *S. aureus* after incubating the bacteria with (a) Au–IgG nanoparticles, (b) unmodified gold nanoparticles, and (c) Au–BSA nanoparticles.

using a Hitachi H-7500 (Tokyo, Japan) and a JEOL JEM-2000 FXII (Tokyo, Japan) instrument. All the UV–visible absorption spectra were obtained using a Varian Cary-50 spectrometer.

RESULTS AND DISCUSSION

Figure 2a presents the TEM image obtained when employing the Au–IgG nanoparticles to probe target bacteria in *S. aureus* solutions. The Au–IgG nanoparticles cover the entire cell surfaces of the *S. aureus* cells, which is not surprising when considering that it has been estimated there are ~ 80 000 binding sites, i.e., protein A units, on the cell wall of an *S. aureus* cell upon which IgG can anchor.⁵ Figure 2b displays the TEM image obtained when employing the unmodified gold nanoparticles to probe target bacteria in an *S. aureus* solution. We observe that only a few gold nanoparticles bind to the cell surfaces of *S. aureus* because of the nonspecific electrostatic interactions between the nanoparticles and the bacteria. To further confirm that the interactions between Au–IgG and *S. aureus* do not arise from nonspecific interactions between the protein-functionized gold nanoparticles and the cell walls of *S. aureus*, we employed Au–BSA nanoparticles as affinity probes to target *S. aureus*. Figure 2c presents the TEM image obtained when employing the Au–BSA nanoparticles to probe target bacteria in an *S. aureus* solution. The cell surfaces of the bacterial cells are free of any nanoparticles, which indicates that BSA does not bind with the cell walls of *S. aureus*. These results confirm that our approach is a successful one for generating effective nanoprobe that allow an examination of the interactions between IgG and its binding sites on the cell surfaces of bacteria.

The M protein on the cell walls of *S. pyogenes* also has been characterized as a binding protein for IgG.¹² Figure 3a presents a

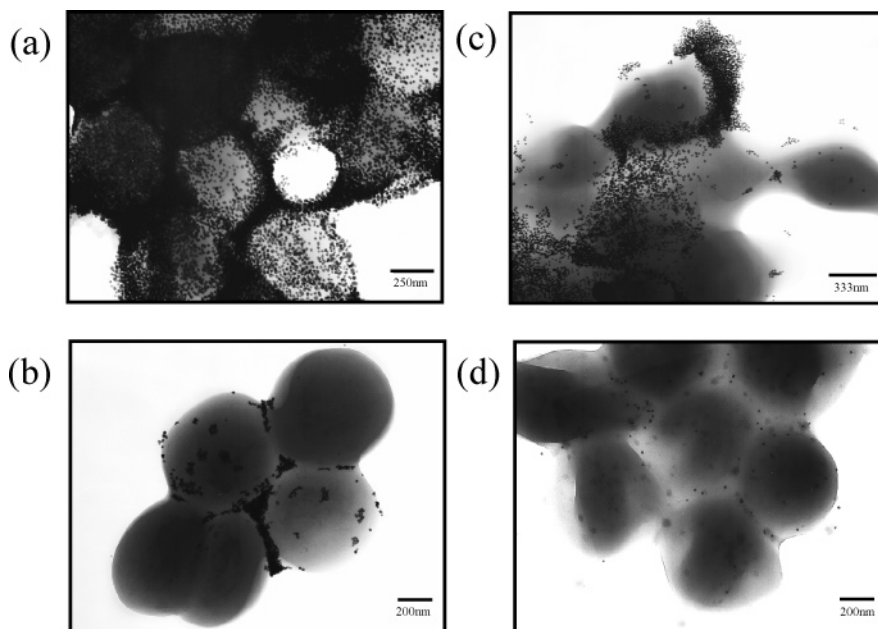


Figure 3. TEM images of *S. pyogenes* JRS4 after incubating these bacteria with (a) Au–IgG nanoparticles and (b) Au–BSA nanoparticles. TEM images of *S. pyogenes* JRS75 after incubating these bacteria with (c) Au–IgG nanoparticles and (d) Au–BSA nanoparticles.

TEM image of *S. pyogenes* (JRS4) in which the bacterial cell surfaces are enveloped with the Au–IgG nanoparticles. For a control experiment, Figure 3b displays a TEM image of *S. pyogenes* (JRS4) obtained after using Au–BSA nanoparticles to probe bacteria in a *S. pyogenes* (JRS4) solution. We observe that only a few nanoparticles have anchored onto the surfaces of the bacterial cells. In contrast, Figure 3c presents a TEM image of JRS75, an M protein-mutated form of *S. pyogenes*, and demonstrates that no Au–IgG nanoparticles are anchored onto its cell walls. Figure 3d displays a TEM image of *S. pyogenes* (JRS75) obtained after using Au–BSA nanoparticles to probe bacteria in an *S. pyogenes* (JRS75)-solution. Similar to Figure 3b, we observe that only a few nanoparticles bind on the surfaces of the bacterial cells. These images indicate that the Au–IgG nanoparticles recognize their binding proteins specifically on the cell walls of *S. pyogenes*.

S. saprophyticus is a pathogen that often infects the urinary tract of young women. To the best of our knowledge, we are unaware of any previous reports that suggest that IgG interacts with the cell surfaces of *S. saprophyticus*, but we believed that our nanoparticles would provide a simple test for whether such interactions exist. To our surprise, the Au–IgG nanoparticles cover the entire surfaces of the cells (Figure 4a), which suggests that IgG has a strong binding affinity for the cell walls of *S. saprophyticus*. To confirm that the interactions between Au–IgG and *S. saprophyticus* do not arise merely from electrostatic interactions between the negatively charged surfaces of the gold nanoparticles and the cell walls of *S. saprophyticus*, we added unmodified gold nanoparticles to the bacterial solution. In this case, Figure 4b displays a TEM image that indicates that the gold nanoparticles do not anchor onto the cell walls of *S. saprophyticus*, but instead, they aggregate together. Figure 4c presents the TEM image obtained after using Au–BSA nanoparticles to probe bacteria in an *S. saprophyticus* solution. We observe that almost no Au–BSA nanoparticles bind to the cell walls of *S. saprophyticus*. These results further confirm the binding specificity between Au–IgG and the cell walls of *S. saprophyticus*.

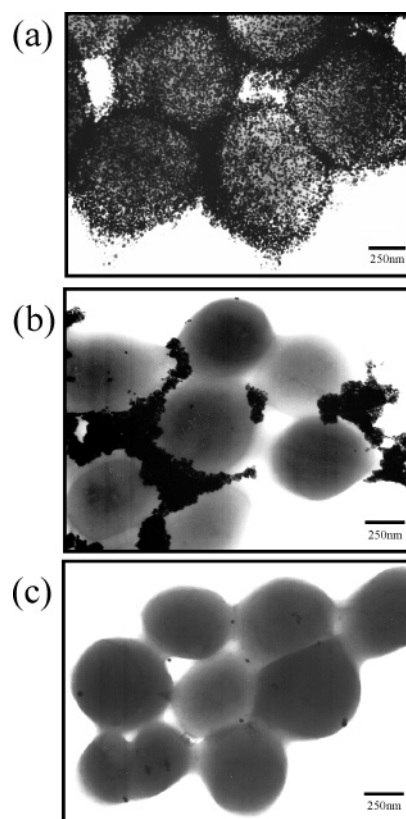


Figure 4. TEM images of *S. saprophyticus* obtained after incubating these bacteria with (a) Au–IgG nanoparticles, (b) unmodified gold nanoparticles, and (c) Au–BSA nanoparticles.

Through the unique characteristics of the *pI* of proteins, we have demonstrated a simple and very straightforward method for attaching functional biomolecules onto the surfaces of gold nanoparticles: i.e., exploiting the electrostatic interactions that exist between the two. Au–IgG nanoparticles prepared this way are capable of recognizing protein A presented by *S. aureus* and

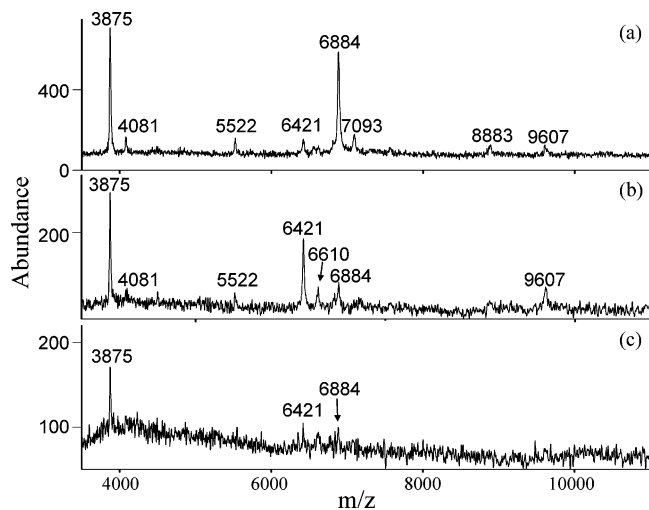


Figure 5. MALDI mass spectra obtained after using Fe–IgG (0.5 mg/mL, 60 μ L) as the affinity probe to selectively concentrate *S. aureus* from aqueous solutions (0.5 mL) at concentrations of (a) 3.85×10^7 , (b) 3.85×10^6 , and (c) 3.85×10^5 cfu/mL.

the M protein presented by *S. pyogenes*. In addition, by applying these IgG-functionalized nanoparticles, we have discovered that the cell surfaces of *S. saprophyticus* contain binding sites that are specific for IgG probes.

We have further immobilized IgG onto the surfaces of Fe₃O₄ magnetic nanoparticles (Fe–IgG) through covalent bonding to generate the Fe–IgG nanoparticles. Upon binding such nanoparticles to their pathogen receptors, the nanoparticle-labeled bacteria may be isolated readily from solution, by using a magnet, and subsequently characterized by MALDI-MS. Panels a–c of Figure 5 present the MALDI mass spectra obtained after using Fe–IgG (0.5 mg/mL, 60 μ L) as the affinity probe to selectively concentrate *S. aureus* at concentrations of 3.85×10^7 , 3.85×10^6 , and 3.85×10^5 cfu/mL, respectively, from aqueous solutions (0.5 mL). The ions at m/z 3875, 4081, 5522, 6421, 6610, 6884, and 9607, which represent *S. aureus*, appear reproducibly in Figure 5a and b. When the concentration of *S. aureus* was decreased to 3.85×10^5 cfu/mL, only the ions at m/z 3875, 6421, and 6884 appear in the mass spectrum (Figure 5c). These results indicate that the Fe–IgG nanoparticles are capable of concentrating target bacteria from aqueous solutions.

Panels a–c of Figure 6 display the MALDI mass spectra obtained after using Fe–IgG (0.5 mg/mL, 60 μ L) as the affinity probe to selectively concentrate *S. saprophyticus* at concentrations of 2.99×10^7 , 2.99×10^6 , and 2.99×10^5 cfu/mL, respectively, from aqueous solutions (0.5 mL). The ions at m/z 3822, 4941, 4988, 6037, 6183, 6393, 6547, 6616, and 6829, which represent *S. saprophyticus*, appear reproducibly in each mass spectrum. We were curious to discover whether live *S. saprophyticus* cells can be selectively recognized by the Fe–IgG nanoparticles. Figure 7 presents the MALDI mass spectrum obtained after using Fe–IgG (0.5 mg/mL, 60 μ L) as the affinity probe to selectively concentrate live *S. saprophyticus* at a concentration of 1.9×10^6 cfu/mL from an aqueous solution (0.5 mL). The ions at m/z 3822, 4988, 6183, 6393, 6616, and 6829 resemble those obtained when applying the heat-killed *S. saprophyticus* cells as the target bacteria (cf. Figure 6). More ions appear at values of $m/z > 7000$ in the spectrum obtained from use of the live bacteria; additional peaks

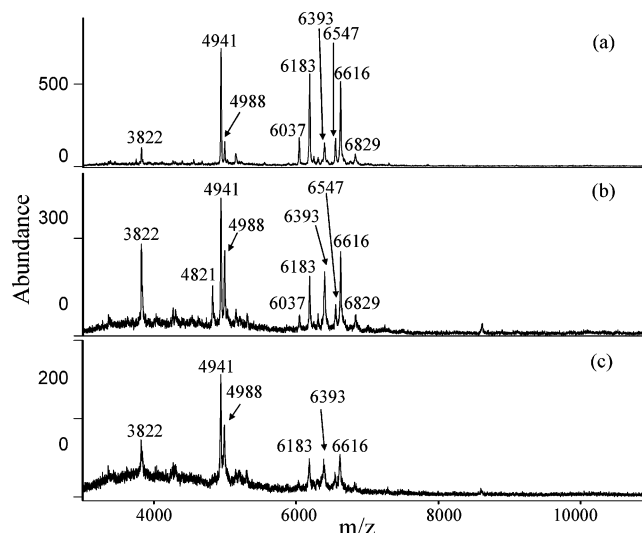


Figure 6. MALDI mass spectra obtained after using Fe–IgG (0.5 mg/mL, 60 μ L) as the affinity probe to selectively concentrate *S. saprophyticus* from aqueous solutions (0.5 mL) at concentrations of (a) 2.99×10^7 , (b) 2.99×10^6 , and (c) 2.99×10^5 cfu/mL.

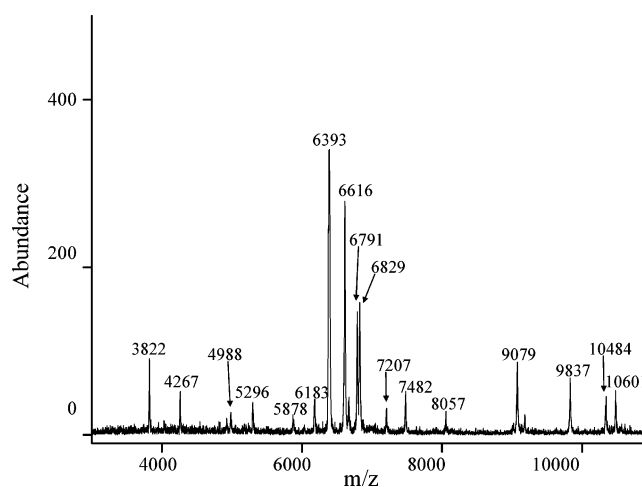


Figure 7. MALDI mass spectrum obtained after using Fe–IgG (0.5 mg/mL, 60 μ L) as the affinity probe to selectively concentrate live *S. saprophyticus* from an aqueous solution (0.5 mL) at a concentration of 1.9×10^6 cfu/mL.

appear at m/z 4267, 5296, 7207, 7482, 8057, 9079, 9837, 10484, and 10601 in the MALDI mass spectrum. These results demonstrate that both live and heat-killed *S. saprophyticus* cells can be trapped selectively by the Fe–IgG probes. Furthermore, the fingerprint ion peaks representing either live or heat-killed *S. saprophyticus* cells resemble one another in the MALDI mass spectra.

We designed an additional probe to investigate whether the Fc region or the Fab region of IgG is the binding site for the cell surfaces of *S. saprophyticus*. We immobilized protein G covalently onto the surfaces of the magnetic nanoparticles to generate Fe–protein G nanoparticles. Protein G is known to be one of the proteins that bind to the Fc region of IgG.⁵ We employed the Fe–protein G nanoparticles to trap IgG and generate Fe–protein G–IgG nanoparticles. The Fab regions of the IgG molecules immobilized on the Fe–protein G nanoparticles must be presented outward because the Fc regions were interacting with the protein G molecules. If the Fc regions of IgG were truly the binding sites

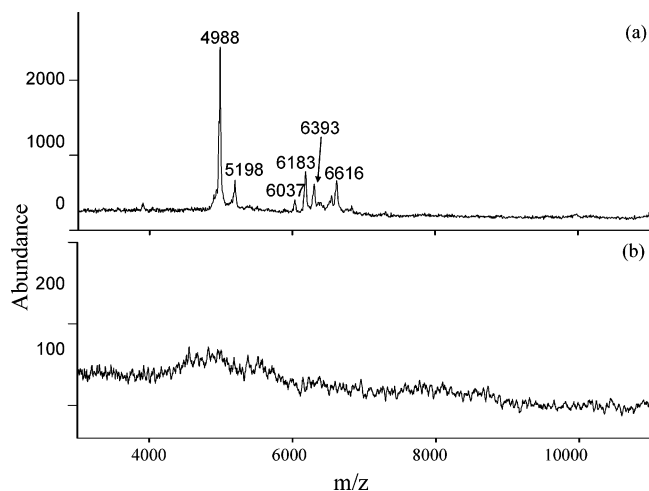


Figure 8. MALDI mass spectra obtained after using the Fe–protein G–IgG nanoparticles as affinity probes to concentrate *S. saprophyticus* from aqueous solutions (0.5 mL) at concentrations of (a) 2.99×10^7 and (b) 2.99×10^6 cfu/mL.

for the cell surfaces of *S. saprophyticus*, then we would expect that the Fe–protein G–IgG nanoparticles would not have any affinity toward the target bacteria. Initially, we used protein A as the target sample to investigate whether we had successfully generated Fe–protein G–IgG nanoparticles that present their Fab regions outward. We expected that the Fe–protein G–IgG species would display no trapping capacity toward protein A because the Fc regions of the IgG molecules interacted with protein G units on the surface of magnetic particles. Therefore, no Fc sites were available to interact with protein A. MALDI MS analysis was employed to characterize the systems after performing the trapping experiments. Our results demonstrate that the Fe–protein G–IgG nanoparticles had no concentrating capacity toward protein A molecules (results not shown), which indicates that we had successfully generated Fe–protein G–IgG nanoparticles presenting their Fab regions outward. The reason we used protein G in place of protein A as the immobilizing linker to attach IgG molecules onto the surfaces of the magnetic nanoparticles was to prevent any possible interference of protein A from the Fe–protein A–IgG nanoparticles during MALDI MS analysis. Panels a and b of Figure 8 present the MALDI mass spectra obtained after using the Fe–protein G–IgG nanoparticles as affinity probes for *S. saprophyticus* at concentrations of 2.99×10^7 and 2.99×10^6 cfu/mL, respectively, from aqueous solutions (0.5 mL). The ions at m/z 4988, 5198, 6037, 6183, and 6616, which represent *S. saprophyticus*, appear in Figure 8a, but none of these ions are observed in Figure 8b. These results indicate that the Fe–protein G–IgG nanoparticles have only a very weak affinity toward *S. saprophyticus* (cf. Figure 6) and confirm our proposed mechanism: i.e., that the Fc region of IgG coordinates at the binding sites on the cell surfaces of *S. saprophyticus*.

Panels a–c of Figure 9 present the MALDI mass spectra obtained after using the Fe–IgG nanoparticles to selectively concentrate *S. saprophyticus* at concentrations of 7.09×10^7 , 2.99×10^7 , and 2.99×10^6 cfu/mL, respectively, from urine samples (0.5 mL). No ions generated from *S. saprophyticus* were observed by direct MALDI-MS analysis of these urine samples (results not shown). In Figure 9a and b, the peaks marked with a B at m/z 4988, 6183, 6393 and 6547 represent ions from *S. saprophyticus*,

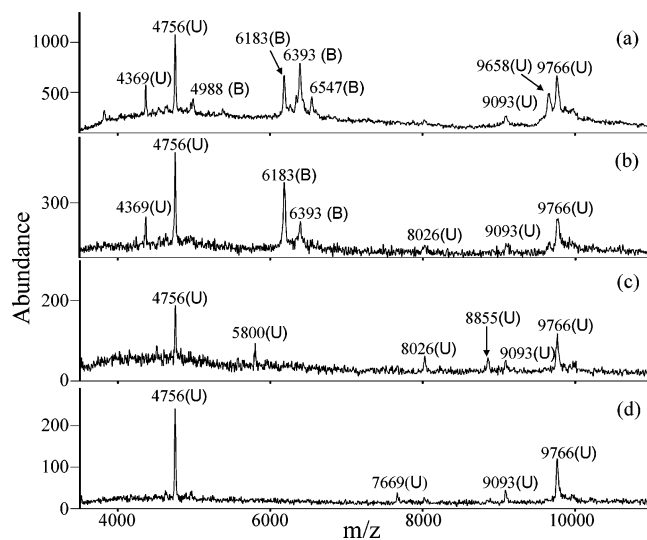


Figure 9. MALDI mass spectra obtained after using the Fe–IgG nanoparticles to selectively concentrate *S. saprophyticus* from urine samples (0.5 mL) at concentrations of (a) 7.09×10^7 , (b) 2.99×10^7 , (c) 2.99×10^6 , and (d) 0 cfu/mL.

while the ions marked with a U were obtained from the urine. When the bacterial concentration of *S. saprophyticus* was lowered to 2.99×10^6 cfu/mL, we observed no ions generated from the bacterial cells in the mass spectrum (Figure 9c). Figure 9d displays the MALDI mass spectrum obtained after using the Fe–IgG nanoparticles as affinity probes to trap target bacteria from a blank urine sample. The peaks at m/z 4756, 9093, 9658, and 9766 appear reproducibly in the MALDI mass spectra of the urine samples. Although the Fe–IgG nanoparticles can concentrate target bacteria selectively from urine samples, the impurities in urine have a significant effect on the capacity of this probe to target bacteria at low concentrations.

CONCLUSIONS

We have demonstrated that Au–IgG nanoparticles can be used successfully to explore the interactions between IgG and the cell surfaces of target bacteria. Furthermore, the Fe–IgG nanoparticles can be used as effective affinity probes to concentrate target bacteria selectively; the microorganism species can then be characterized by using MALDI-MS. When these nanoscale probes are employed to concentrate traces of bacterial cells from urine samples, however, interference from the urine impurities can affect the binding capacity of the Fe–IgG probes. This technology may provide a potential benefit to the rapid identification of pathogens, but further improvements are necessary to effectively reduce the interference from impurities in urine and to render this approach as a sensitive one for analyzing samples obtained from biological fluids.

ACKNOWLEDGMENT

We thank the National Science Council (NSC) of Taiwan for supporting this research financially. We also thank Dr. Hsin-Tien Chiu's group for technical assistance in obtaining the TEM images.

Received for review September 3, 2004. Accepted November 2, 2004.

AC048688B